

Colorimetric Transition of Polydiacetylene/Cyclodextrin Supramolecular Assemblies and Implications as Colorimetric Sensors for Food Phenolic Antioxidants

Riccardo Sergi, Benedetta Brugnoli, Elisa Sturabotti, Antonella Piozzi, Luciano Galantini, Vincenzo Taresco, and Iolanda Francolini*

Molecular self-assembly has significant potential in the field of sensing. Polydiacetylenes (PDAs) are conjugated polymers possessing peculiar optical properties obtained by photopolymerization of self-assembled diacetylene monomers. Herein, the blue-to-red phase transition upon either thermal stimulus or interaction with cyclodextrins (CDs) of two PDAs, bearing either carboxylic (PCDA) or amino (PCDA-NH₂) polar heads, is investigated to develop a colorimetric sensor for food phenolic antioxidants. The change in the PDA polar head does not affect significantly thermo-chromatic transition. Upon thermal stimulus, in both PDAs, color transition occurs straightforward between two distinct stable states and does not involve the disordering of the PDA crystal phase, as revealed by UV-vis spectroscopy and SAXS analysis. Contrarily, PDA/ α -CD interaction is influenced by intermolecular forces among PDA polar heads and is more efficient for PCDA. α -CDs presumably cause changes in both PDA backbone conformation and local environment surrounding the individual PDA chains. The PCDA/ α -CD assemblies are investigated as colorimetric sensors for the detection of Tyrosol (Ty) and caffeic acid (CAF), by using the principle of competitive inclusion complex formation. The system results to be more sensitive to CAF than Ty and may permit the determination of CAF in concentration ranges suitable for different food products.

1. Introduction

The bottom-up design and generation of complex molecular systems through spontaneous association of molecules is an exciting challenge in the nanotechnology field.^[1] Self-assembly, the process by which molecules spontaneously organize into well-defined structures, is at the heart of this approach. One example of a self-assembling system is given by amphiphilic molecules, which can establish various intermolecular interactions, such as polar-polar interactions, van der Waals interactions, and directional hydrogen bonds, leading to the formation of well-defined structures.^[2,3] Molecular self-assembly is a fundamental concept that is prevalent in many fields of study, including chemistry, physics, biology, and materials science.^[4-6]


Supramolecular assemblies, which are composed of multi-component systems aggregated by noncovalent bonds, may exhibit unique properties and functions that cannot be predicted from the features of the original constituents.^[7] By rationally designing the colloidal entities and

interfaces and controlling the specific interactions between them, it is possible to tune the hierarchical self-assembly of supramolecular assemblies.^[8] This approach can be used to create structures such as adaptive colloidal molecules and crystalline organizations. The size, shape, and interactions between different colloidal building blocks can be varied to create diverse structures with specific properties and functions.^[9] This allows for the creation of novel materials with tailored properties and the development of nanoscale devices and sensors.

In this regard, the principle of molecular self-assembly has significant potential in the field of sensing.^[10] In a self-assembled sensing system, the sensing element is designed to respond to a specific molecular target by undergoing a conformational change that results in a detectable signal.^[11] This can be achieved through the incorporation of molecular recognition elements, such as specific receptors or ligands, into the self-assembling system. The presence of the target molecule leads to the formation of a stable complex that alters the self-assembled structure and generates a measurable signal, such as a change in color or

R. Sergi, B. Brugnoli, E. Sturabotti, A. Piozzi, L. Galantini, I. Francolini
 Department of Chemistry
 Sapienza University of Rome
 P.le A. Moro, Rome 5-00185, Italy
 E-mail: iolanda.francolini@uniroma1.it

V. Taresco
 School of Chemistry
 The University of Nottingham
 Nottingham, NG7 2RD, UK

 The ORCID identification number(s) for the author(s) of this article can be found under <https://doi.org/10.1002/macp.202300098>

© 2023 The Authors. Macromolecular Chemistry and Physics published by Wiley-VCH GmbH. This is an open access article under the terms of the Creative Commons Attribution License, which permits use, distribution and reproduction in any medium, provided the original work is properly cited.

DOI: 10.1002/macp.202300098

fluorescence intensity.^[12] Self-assembled sensing systems offer several advantages over traditional sensing methods. They can be designed to be highly selective and sensitive to specific molecular targets, and they can operate in complex environments, such as biological samples or environmental matrices.^[13]

Polydiacetylene (PDA) assemblies, either dispersed in solution as nanostructures or surface-attached layers (Langmuir–Blodgett films), are an attractive platform for developing colorimetric sensors.^[14] PDAs are conjugated polymers obtained by 1,4 addition reaction of self-assembled diacetylene (DA) monomers induced by UV irradiation. Thanks to their delocalized network of π electrons, which results from the conjugation of the alternating ene-yne groups, they have strong absorption in the visible region of the spectrum with a maximum absorption peak at 640 nm (blue-phase).^[15] Stimulation of blue phase PDA with heat, pH, mechanical stress, chemical recognition events can induce perturbations and conformational rotation of the PDA's ene-yne backbone and a color shift to red phase (maximum absorption wavelength around 550 nm). This colorimetric response is highly visible and can be directly observed by the naked eye, in a "litmus test" fashion. The red-phase of PDAs also exhibits interesting fluorescent properties and is highly applicable in fluorescence-based sensor systems.^[16] These unique optical properties, along with the ease of chemical modification of their hydrophilic heads and the remarkable stability, render PDAs a captivating field of investigation. They hold potential for advancing our understanding of conjugated polymers on a fundamental level, while also offering practical applications in diverse areas such as environmental monitoring, medical diagnosis, and food safety, particularly in sensing and imaging applications.^[17–21] Specifically, PDA-based sensors have garnered significant attention in the realm of food applications. These sensors are renowned for providing a cost-effective, versatile, and user-friendly approach to monitor the chemical composition of food or detect the presence of harmful contaminants. The pronounced colorimetric signal of PDA sensors can be easily read by consumers and workers without technical training, making them ideal for use in the food industry.^[21]

Cyclodextrins have been used as guest molecules to induce changes in the PDAs' structure and resulting optical properties.^[22,23] Alpha-cyclodextrins (α -CDs) were demonstrated to be able to induce color transition in photopolymerized self-assembled 10,12-pentacosadiynoic acid (PCDA), a diacetylene monomer bearing a carboxylic group polar head.^[22,23] Studies using 4-nitrophenol as an inhibitor supported the hypothesis that the PDA color-transition induced by α -CDs was due to the formation of inclusion complexes with the polydiacetylene chain.^[22] This property has potential applications in the development of colorimetric sensors for various analytes, and, so far, it has been exploited to develop sensors for wastewater pollutants.^[24]

Despite the general understanding of the mechanism of PDA blue-to-red color transition, a clear picture of how a large variety of different stimuli causes this transition is often lacking. In order to broaden the basic knowledge on PDA/CD supramolecular interactions as well as to investigate further the use of CDs as transducer molecules for PDA-based sensors, in this study, the color-transition behavior of two PDA systems, obtained respectively from the commercial PCDA and its amino-functionalized derivative (PCDA-NH₂), was examined in response to thermal stimulus and interaction with α -CDs and β -CDs. The effect of

changes in the PDA polar head on its colorimetric transition was investigated by UV-vis spectroscopy and Small Angle X-ray Spectroscopy. Implications on the use of such supramolecular assemblies to develop a colorimetric sensor for the detection of phenolic antioxidant compounds in food products was examined. Ty and CAF were chosen as model phenolic antioxidants because commonly found in fruits, vegetables, and beverages, and known for their preventive and disease-fighting properties. Specifically, the inhibition of colorimetric transition of PDAs induced by α -CD due to competitive interaction with the two selected phenols was studied. Interestingly, an indirect colorimetric determination of CAF was possible and, overall, the obtained results highlight how PDA/CD may provide a simple and rapid detection method for antioxidants in food products and agricultural byproducts.

2. Results and Discussion

Phenolic- and polyphenolic-rich foods are known to afford protection against the development of cardiovascular and degenerative diseases, cancer, and diabetes.^[25] Foods that are particularly rich in phenols include fruits (apples, cherries, grapes, oranges, peaches, pears, plums), nuts and seeds, whole grains and beverages, like coffee, tea, red wine.

Changes in phenolic content in these food products is considered an indicator in the food quality.^[26] Efforts are being devoted to the development of rapid methods for analysis of phenolic compounds in beverages and grains.^[27]

A common phenolic compound abundant in coffee and tea but also present in red wine is CAF.^[28] CAF is a hydroxycinnamic acid endowed with potent antioxidant activity,^[29] which may help to protect against oxidative stress and reduce the risk of chronic diseases. It has also been shown to have anti-inflammatory effects and anticancer property.

Ty is an abundant phenol in olive oil mill wastewater and, in spite of its weak antioxidant activity,^[30] Ty was found to be effective in preserving cellular antioxidant defenses, probably by intracellular accumulation.^[31]

Herein, the possibility to use PDA/CDs assemblies to detect these two phenols was investigated. CDs are intriguing molecules, which can form inclusion complexes with a variety of guest molecules. This property makes them attractive model systems for studying ligand-receptor interactions and host-guest chemistry.

2.1. Synthesis and Characterization of the Amino-Functionalized DA Monomer (PCDA-NH₂)

In order to investigate the effect of different head groups of the DA monomer on the interactions with α -CDs and β -CDs, the acidic DA monomer PCDA was derivatized with amino groups by activation of its carboxylic group with a carbodiimide followed by amidation with ethylenediamine (EDA) (Figure 1). Both the activated PCDA-NHS and amidated PCDA-NH₂ products were characterized by ATR-FTIR and ¹H-NMR. The spectroscopic analysis of PCDA-NHS is reported in Supporting information (Figures S1 and S2) while in Figure 2 the ATR-FTIR and ¹H-NMR spectra of PCDA and PCDA-NH₂ are reported, respectively.

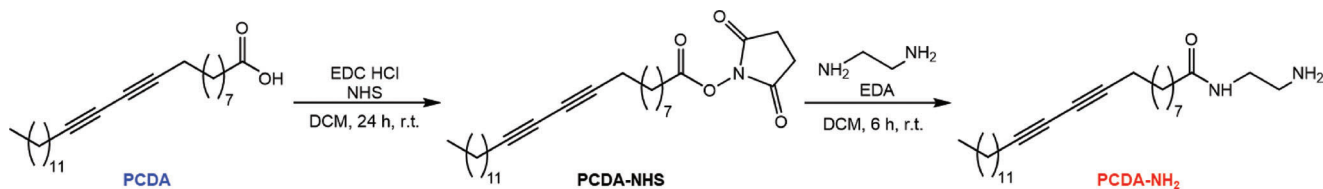


Figure 1. Reaction scheme for PCDA derivatization with EDA to obtain the amino-functionalized diacetylene monomer PCDA-NH₂. Amidation is carried out on the activated ester intermediate PCDA-NHS.

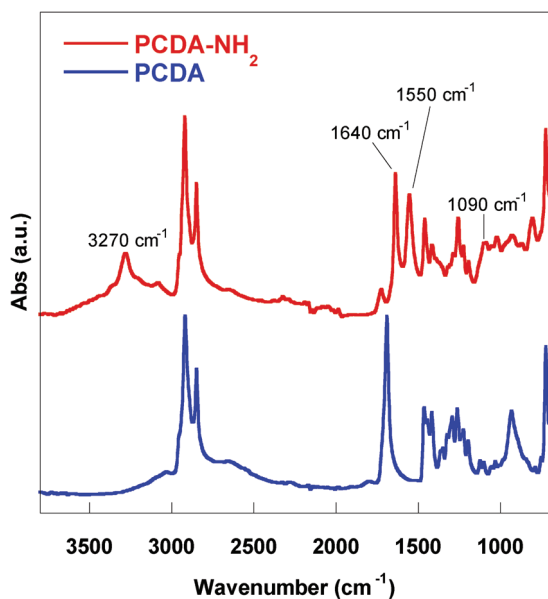


Figure 2. ATR-FTIR spectra of PCDA (in blue) and the amino-functionalized PCDA-NH₂ (in red).

In the ATR-FTIR spectrum of PCDA-NH₂, the new adsorption peak at 3270 cm⁻¹ related to the amide N–H stretching can be observed. Furthermore, the amidic bond, which resonates at 1640 cm⁻¹ (amide I), and at 1550 cm⁻¹ (amide II), together with the C–N stretching at 1090 cm⁻¹, confirmed the success of the amidation reaction.

As for ¹H-NMR analysis in the PCDA spectrum (Figure 3A), the triplet at 0.9 is associated to the methyl group at the end of pentacosadiynoic acid while the broad and intense signal between 1.4 and 1.2 ppm is related to the thirteen methylene groups in the chain. The -CH₂ in α and β to the triple bonds give a triplet and a quintet at 2.2 and 1.5 ppm, respectively. Lastly, methylene groups adjacent to the COOH fall at 2.3 and 1.6 ppm, as triplets.

The amidation of EDA with PCDA is visible through the appearance of two new peaks at $\delta = 3.3$ and 2.9 ppm (triplet) in the PCDA-NH₂ spectrum (Figure 3B). The signals are related to the methylene groups of EDA unit, in α and β to the amidic nitrogen respectively. Furthermore, the amidic proton contributes to the spectrum with a broad singlet centered at $\delta = 6$ ppm.

Elemental analysis, ¹³C-NMR spectroscopy and high-resolution mass spectroscopy further confirmed the obtainment of the product (Table S1, Figure S3 and Figure S4, Supporting Information)

2.2. Thermal Properties of DA Monomers

The influence of structural change on the strength of intermolecular interactions in the two DA monomers was investigated by DSC and TGA analyses.

From the DSC curves obtained from the second heating cycle (Figure 4A), it can be observed that PCDA has a sharp melting peak at 67 °C with a heat of fusion (ΔH_m) of ≈ 102 J g⁻¹. When the DA head group is varied, the melting behavior of the DA monomer changes significantly. The amino-derived PCDA-NH₂, despite having the same alkyl tail as PCDA, shows a broad endothermic band between 40 and 100 °C with a ΔH_m value of 50 J g⁻¹ (Figure 4A). This suggests that PCDA-NH₂ has a less ordered structure than PCDA. Similar findings were reported by Charoenthai and colleagues, who proposed the presence of a liquid crystal (LC) phase induced by hydrogen bonds among the amido and amino head groups, which increase molecular rigidity.^[32] Analogous thermal behavior was observed for other types of DA monomers having head groups strongly interacting each other.^[33] The less ordered structure of PCDA-NH₂ can justify its lower thermal stability compared to PCDA as evidenced by the thermogravimetric analysis (Figure 4B). This finding is not surprising and aligns with DSC analysis, which suggests a lower crystallinity of PCDA-NH₂, and with the colorimetric response upon T stimulus (see in the next section), where PCDA-NH₂ shows an earlier transition. Unlike PCDA, PCDA-NH₂ shows a continues and more rapid weight loss up to 200 °C, presumably related to the presence of adsorbed water. The higher hydrophilicity of PCDA-NH₂ compared to PCDA could be related to the higher number of hydrogen bonding sites present in this molecule.

2.3. Size and Zeta Potential

Self-assembling of the PCDA and PCDA-NH₂ diacetylene monomers in water was induced by nanoprecipitation. Then, the DA suspensions were photopolymerized to obtain blue-colored PDA nanoaggregates (Figure 5A), polyPCDA and polyPCDA-NH₂, endowed with carboxylic and amino groups, respectively. Dynamic light scattering and zeta potential (ζ) measurements were performed (Figure 5B). The DLS size distribution curves are reported in Supporting Information (Figure S5). In Figure 5C, the H-bond interactions among the polar heads of the two PDAs are evidenced.

The polyPCDA sample showed the lowest size (183 nm) and a quite negative zeta potential (–55 mV) suggesting a good stability of the suspension. A slight increase in size, from 183 to 232 nm, was registered after PCDA derivatization and, also, the zeta

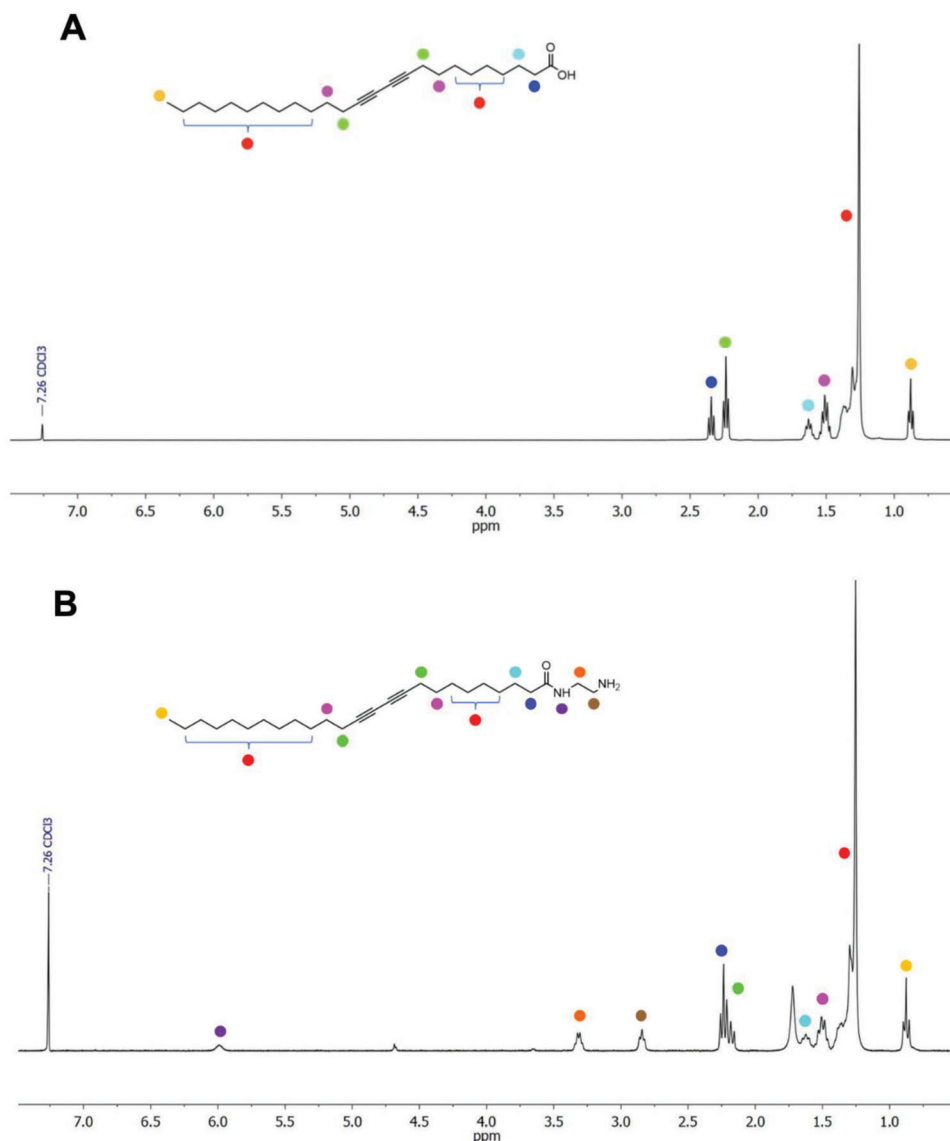


Figure 3. $^1\text{H-NMR}$ spectra of A) PCDA and B) PCDA- NH_2 in CDCl_3 . Colored dots indicate the moieties in the two compounds.

potential became positive (+43 mV), thus further confirming the presence of amino polar heads.

2.4. Colorimetric Response of PDAs upon Thermal Stimulus

PDAs' colorimetric response was investigated upon thermal stimulus. **Figure 6A,B** shows the UV–vis spectra of polyPCDA and polyPCDA- NH_2 at different temperatures. As it can be observed, at 25 °C, before the heating cycle, the spectrum of polyPCDA blue suspension presents a maximum absorbance at 640 nm. Upon heating, the maximum absorbance is shifted to lower wavelengths, and the absorbance intensity at 640 nm coherently decreased. At 60 °C, the absorbance at 540 nm reached a maximum with the complete disappearance of the peak at 640 nm, and the color turned visually red. Interestingly, in **Figure 6A,B**, it can be observed the formation of an isosbestic

point, indicating that the phase change from red to blue occurred without formation of intermediate colored phases. That was found also for polyPCDA- NH_2 vesicles (**Figure 6B**). A similar observation has been reported for the blue form of annealed Langmuir–Blodgett films of cadmium 10,12-tricosadiynoate.^[34] The isosbestic point suggests that the blue and the red forms exist in distinct stable states (the two chromatic phases), with a complementarity between both forms.

Plots of colorimetric responses of PDAs as a function of temperature often provides useful information about the thermochromic properties of the polymer.^[35] **Figure 7** shows the CR (%) as a function of T for polyPCDA and polyPCDA- NH_2 . Both PDAs have characteristic temperature range over which the CR values sharply increase. The temperature ranges are similar for the two systems (30–55 °C) but the temperature corresponding to CR = 50% was found to be different and equal to $(43 \pm 1)^\circ\text{C}$ for polyPCDA and $(38 \pm 1)^\circ\text{C}$ for polyPCDA- NH_2 . It is possible

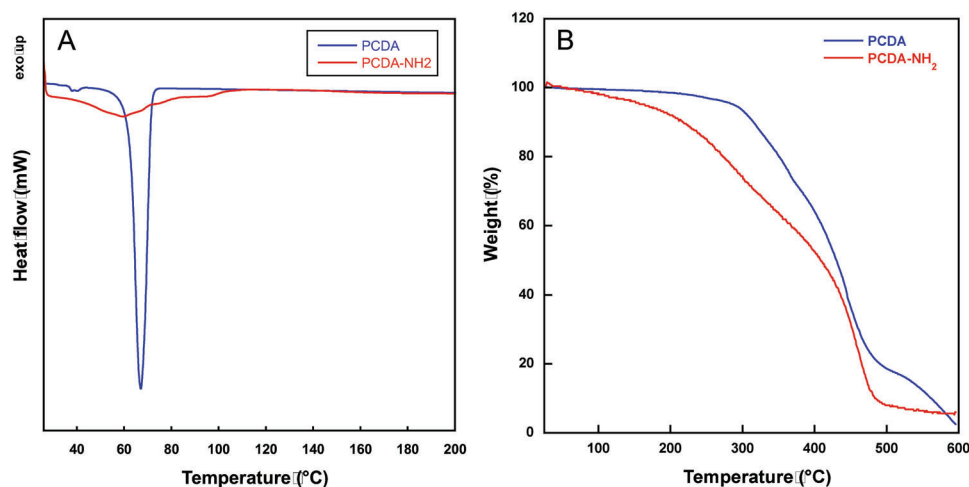


Figure 4. A) DSC and B) TGA curves for PCDA and PCDA-NH₂ monomers.

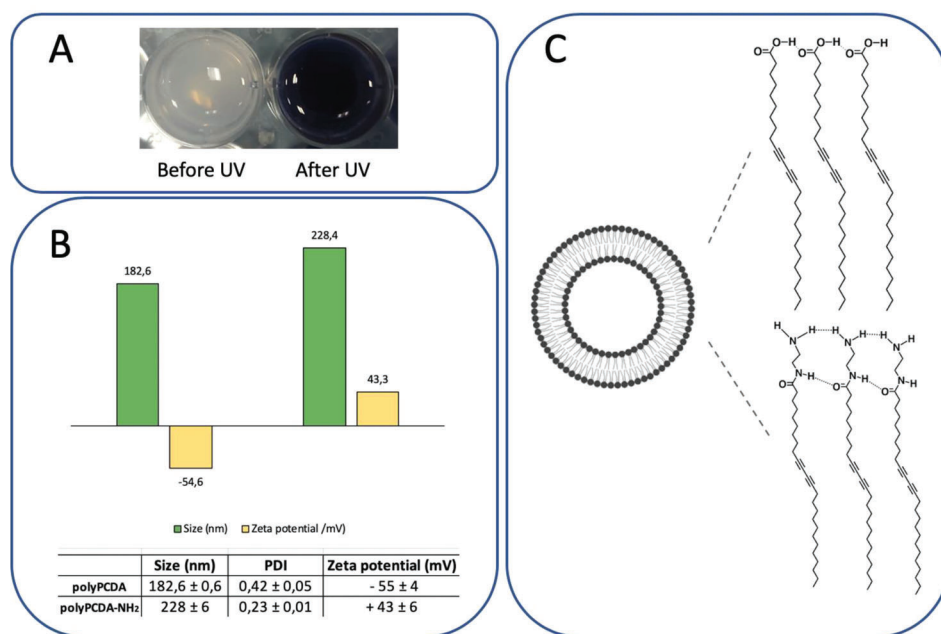


Figure 5. A) PCDA-NH₂ suspension before (white) and after photopolymerization (blue); B) Size and zeta potential of polyPCDA and polyPCDA-NH₂; C) PDA vesicles showing H-bond interactions among the polar chains.

that the sensitivity of the color transition of PDAs is related to differences in intermolecular forces among the two types of PDAs. This is consistent with thermal analysis carried out on the corresponding DA monomers, which provided evidence of these differences.

While it is well-known that the PDA blue form can be altered to the red one upon temperature increase^[15], the mechanism of the phase transition of the PDA thermochromism still deserves investigation. The most accredited mechanism model envisages that the variation of the energy *I* of the $\pi - \pi^*$ transition in PDAs is related to changes in the conformation of the polymer backbone as well as to changes in the local environment surrounding the backbone.^[36] As the conformation becomes more dis-

torted, twisted and non-planar, the level of electron delocalization decreases, increasing the *E* value. Chains in the blue single-crystal phases are known to be planar with the so-called “ene-yne” bond alternation.^[37,38] However, the conformation of red chains has been debated, and there is still no general agreement on that. Previous studies by infrared and Raman spectroscopy evidenced an increased disorder during the blue-to-red transition, suggesting that the blue solid-state polymer turns into red because of a crystal-to-amorphous transition (melting of the alkyl side chains).^[39–41] However, other studies evidenced a local increase of order during color transition suggesting that the formation of the red phase is not related to a decrease of order, as often claimed.^[42,43] According to these latter two cited studies, the red

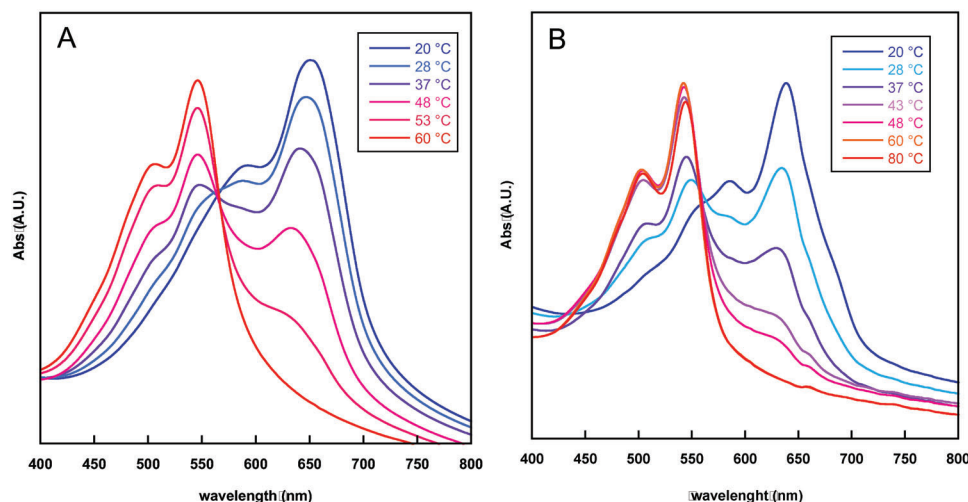


Figure 6. UV-vis spectra of A) polyPCDA vesicles and B) polyPCDA-NH₂ at different T.

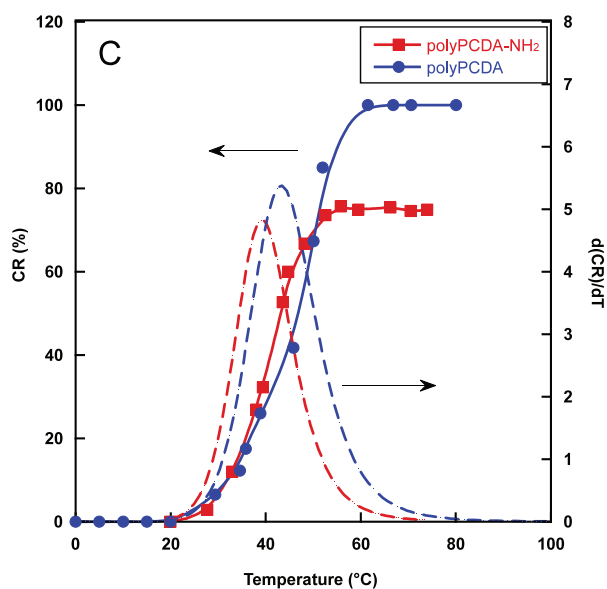


Figure 7. Colorimetric response (CR, %) of polyPCDA and polyPCDA-NH₂ as a function of T.

phase is not inevitably disordered. The different transition energies of the blue and red forms are supposed to reflect different geometries of the chains.

The SAXS analysis performed in this study on polyPCDA, chosen because responding to α -cyclodextrin in a stronger fashion (see section 2.4), before and after stimulus at increasing temperatures (Figure 8) supports the hypothesis of a color transition that does not involve the disordering of the crystal blue phase. As shown in Figure 7, the scattering profiles of the polyPCDA blue form (35 °C) showed a single reflection peak at a d -spacing of ≈ 5.1 nm. By considering the chain length of the investigated DA monomer and the q^{-2} slope at low scattering angle typical of a planar structure, presumably, PDA is assembled in a lamellar phase with tilted and partially interdigitated chains. Upon thermal stimulus up to 75 °C (red form), an asymmetric broaden-

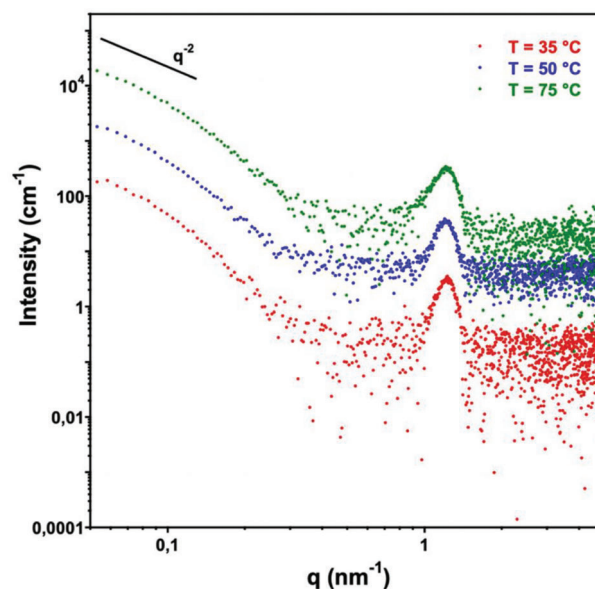


Figure 8. SAXS analysis of polyPCDA at 35, 50 and 75 °C. The plot reports the experimental scattering profiles on absolute scale. Curves have been arbitrarily shifted on the intensity axis by a suitable factor to avoid data overlap and help visualization. The q^{-2} slope at low scattering angles is reported as expected for a lamellar structure.

ing of the reflection peak toward lower scattering angles was observed (Figure 8). Kuriyama et al. assigned this peak to the longitudinal spacing of PDA Langmuir Blodgett.^[34] They also observed that an increase of this spacing occurred upon transition from the blue to the red forms. We suggest that the observed peak is related to the interlamellar spacing of the multi lamellar aggregates formed by PDA. The observed asymmetric broadening toward lower q values, shows that a lowering of the order as well as an increase of this spacing occurs on average upon the thermal induced transition. Apparently, both the blue and red forms have a relatively similar ordered structure in the hydrocarbon side chain and that the degree of conformational order is only

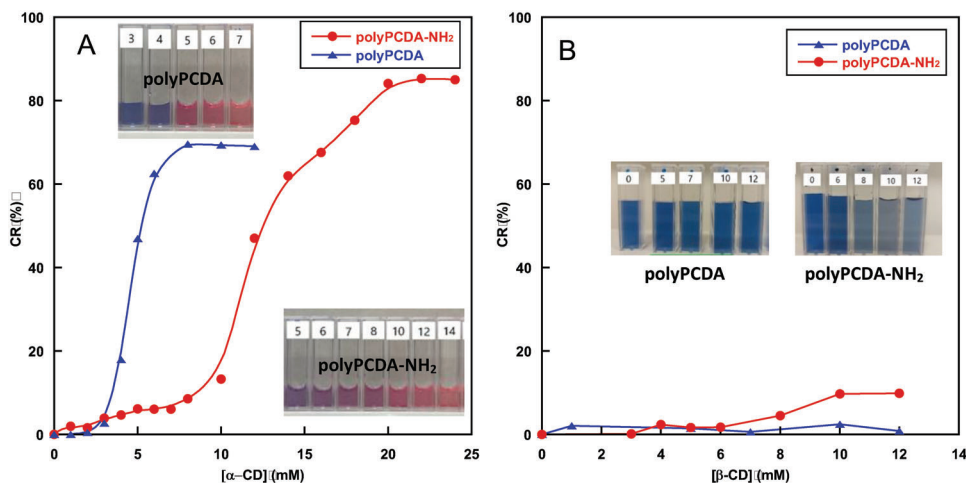


Figure 9. Colorimetric response (CR, %) of polyPCDA and polyPCDA-NH₂ induced by α -CDs (A) or β -CDs (B) concentration increase.

partially influenced by the thermal treatment. As suggested by Campbell and Davies,^[44] change in the energy of the PDA backbone exciton may be related to a change in the inter-backbone spacing within the crystals, rather than to an increase of the conformational disordering of the hydrocarbon side chain.

2.5. Polydiacetylene/Cyclodextrin Supramolecular Assemblies

The possible effects of α -CDs and β -CDs on the structure and color-transition of the two photopolymerized PDAs was investigated. It is already known that PCDA undergoes a blue-to-red color transition by interaction with α -CDs but not with β -CDs.^[22] In this study, the CR (%) of PDA/CD supramolecular assemblies based on polyPCDA or polyPCDA-NH₂ was compared and changes occurring in the molecular structures of PDAs during the blue-to-red color transition caused by α -CDs (or β -CDs) concentration increase were studied. As displayed in Figure 9A,B, only α -CDs caused a color transition in both the two investigated systems. β -CDs interaction did not cause any detectable color change.

α -CDs promoted a sharp blue-to-red color transition of the polyPCDA vesicles in the 4–6 mM α -CD concentration range. The color transition was found to be less abrupt for polyPCDA-NH₂ vesicles, where a gradual increase of CR (%) was observed starting from \approx 5 mM α -CD concentration up to \approx 20 mM where the maximum response was obtained. This gradual transition of polyPCDA-NH₂ is also evident from the images of the PDAs solutions challenged with increasing α -CD concentrations reported in the insets of Figure 9A. The PDA color transition upon α -CD interaction is presumably induced by the formation of an inclusion complex between the inner cavity of α -CD and the hydrophobic ordered alkyl chains of PDA, as previously hypothesized.^[22] This complexation induces alteration of the polymer conformation that ultimately influences its electronic properties and gives rise to the color transition. Considering the diameters of the cyclodextrins, as well as the inter-chain distance in PDA, it is reasonable that α -CD is superior to β -CD due to their structural differences. Specifically, the outer diameters of CDs are 1.37 and

1.53 nm for α and β -CD,^[45] respectively, while the inter-chain distance in PCDA is \approx 0.5 nm.^[46] Presumably, the smaller diameter of α -CD makes it more capable of penetrating the inter-chain gaps in PDA compared to β -CD.

To determine the affinity between PDAs and α -CDs, ΔA_{640} values were reported as a function of α -CD concentration (Figure S6, Supporting Information) and fit with the Hill equation, usually employed to investigate the interaction between ligands and proteins.^[47] From the Hill plot (Figure S6, Supporting Information), the apparent dissociation constants K_d were determined for the two systems. Specifically, $K_d = (4.2 \pm 0.1) \times 10^{-3} \text{ M}^{-1}$ and $K_d = (10.7 \pm 0.3) \times 10^{-3} \text{ M}^{-1}$ were found for polyPCDA and polyPCDA-NH₂, respectively, evidencing that polyPCDA has a better affinity for α -CD than polyPCDA-NH₂. This finding is coherent with a polyPCDA color transition at lower α -CD concentration (4–6 mM) compared to the one of polyPCDA-NH₂ (10–20 mM).

Interestingly, contrarily to the PDAs' color-transition behavior upon thermal stimulus, it was not observed an isosbestic point in the PDAs' UV-vis spectra recorded at different α -CD concentrations (Figure S7, Supporting Information). This indicates that the chromatic phase transition is not straightforward between two stable forms. It seems reasonable that the transition induced by PDA/ α -CD interaction is more complicated than that induced by thermal stimulus. α -CDs may interact at different levels with PDA chains exposed on the surface. The intermolecular forces among the individual PDA chains affect the interaction. In the polyPCDA-NH₂ system, the formation of two hydrogen bonds between head groups (Figure 5C), instead of one H-bond in polyPCDA, can cause an increase in molecular rigidity, which may limit the interaction with α -CD and the formation of the inclusion complex.

The complicated phase change induced by α -CDs, which lacks the isosbestic point, may be related to two phenomena. α -CDs interaction not only may cause a change in conformation of the polymer backbone but also change the local environment surrounding the individual PDA chains. Therefore, the variation of the overall energy (E) of the $\pi - \pi^*$ transition is presumably related to both changes in the energy level of the repeat unit molecule defined by the resonance backbone conformation and

changes in the degree of the electrostatic interactions among the dipole moments on the individual chains affecting the resonance backbone structure. A similar hypothesis was invoked to justify the lack in the isosbestic point during color transition of the bluish-green form obtained by the photopolymerization of annealed cadmium 10,12-tricosadiynoate Langmuir–Blodgett films.^[34]

To study structural changes during the blue-to-red color transition induced by α -CDs, SAXS analysis was performed on polyPCDA exposed to different α -CD concentrations (Figure S8, Supporting information). As it can be observed, the reflection peak at d -spacing of ≈ 5.1 nm of the polyPCDA crystal structure is not observable after α -CD interaction at all concentrations. We cannot exclude that the α -CD scattering profiles cover the polyPCDA signals, even if subtraction of the scattering of the only CDs from the total scattering still does not permit to reveal the PDA reflection peak. It is not trivial to univocally attribute the absence of the PDA reflection peak to a disordering of the PDA alkyl chains upon interaction with α -CDs. Further investigations are definitely needed. However, this phenomenon could occur and would be consistent with the lack in the isosbestic point, which supports a change in the local environment surrounding the individual PDA chains. Indeed, it is reasonable that the breaking of the interactions among PDA chains occurs in favor of the establishment of PDA/ α -CD interactions.

2.6. Use of PDA/CD Assemblies for Detection of Tyrosol and Caffeic Acid

As a proof of concept, polyPCDA/ α -CDs supramolecular assemblies were investigated as colorimetric sensors for phenolic compounds by using the principle of competitive inclusion complex formation. CAF and Ty were chosen as model phenolic antioxidants because of their relevance in food products. While it is known that CAF forms inclusion complexes with α -CDs,^[46] we investigated such ability for Ty by studying the thermal behavior of α -CD/Ty mixtures at different molar ratios. An endothermic peak due to melting at 95 °C ($\Delta H_m = 207$ J/g) was observed for pure Ty (Figure S9, Supporting Information). A progressive reduction in the melting enthalpy of Ty with the increase in α -CD/Ty molar ratio was observed suggesting the formation of α -CD/Ty complexes. Also, a shift of the peak at lower temperature was observed. The peak was substantially reduced at α -CD/Ty 1/1 molar ratio ($H_m = 28$ J/g) and disappeared at α -CD/Ty 2/1 molar ratio. Similarly to α -CD/caffeic acid mixtures, the formation of inclusion complexes can be hypothesized.^[48]

Such ability of α -CDs to complex Ty and CAF was used to inhibit polyPCDA/ α -CD complex formation and related blue-to-red color transition, in order to detect phenolic antioxidants. The polyPCDA system was chosen because of its higher affinity to CD, as shown by the colorimetric response (Figure 9) and Hill plot (Figure S6, Supporting Information).

Figure 10 illustrates CR' (%) of polyPCDA/ α -CD (8 mM) after exposure to the two investigated phenolic antioxidants.

As described in the experimental section, CR' (%) was used to quantify the polyPCDA blue phase which did not form inclusion complex with α -CD. CR' (%) increases with the increase in the concentration of phenolic compounds. Indeed, for phe-

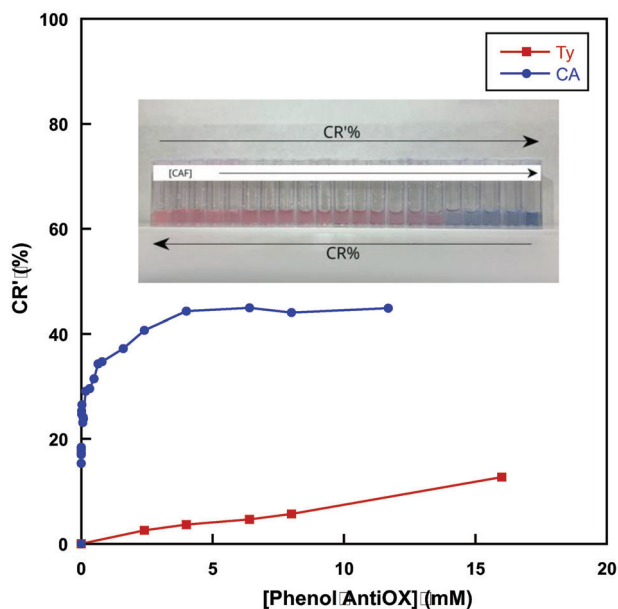


Figure 10. Colorimetric response of polyPCDA/ α -CD (8 mM) after exposure to CAF Ty. In the inset of the figure, the change of the polyPCDA suspension color from red to blue with increasing CAF concentration is shown.

Table 1. Correlation between the range of colors of the polyPCDA/ α -CD suspensions and CAF concentration. Examples of food products containing caffeic acid in concentration ranges suitable for detection.

	Color range	CAF concentration range, mg/100 mL (μ M)	Food
1	Light pink	≤ 0.115 (6.4)	EVO oil
2	Dark pink	0.115 (6.4) < [CAF] ≤ 5.76 (320)	EVO oil, fruit juices, red wine
3	Light purple	5.76 (320) < [CAF] ≤ 14.4 (800)	Coffee beans, red wine
4	Blue	14.4 (800) < [CAF] ≤ 19.2 (2400)	Coffee beans

nol concentration equal to zero, α -CDs are available for interaction with polyPCDA and can induce color transition from blue to red (red suspension, CR' (%) = 0). For variable concentrations of phenol, α -CDs are either partially or not available for interaction with polyPCDA and can induce a reduced or no color transition (blue suspension). According to the extent of color transition, it is, therefore, possible to determine phenol content. The developed polyPCDA/ α -CD was shown to be more sensitive to CAF than Ty, as evidenced by the rapid increase in CR' (%) already at low CAF concentrations. Also, the maximum value of CR' (%) was greater for CAF ($\approx 45\%$) than Ty ($\approx 15\%$). A potential explanation of this behavior is the different stability of the two α -CD/phenol complexes in presence of polyPCDA. Dissociation of the α -CD/tyrosol complex presumably occurs upon contact with polyPCDA suspension because of the α -CD better affinity for polyPCDA than Ty.

A linear response was found in the 0.8–800 μ M CAF concentration range with a Limit of Detection (LOD) of 680 μ M. According to the naked eye color scale (Inset of Figure 10), it is possible to identify 4 color ranges (Table 1).

CAF elicits several interesting and various biological responses, such as antibacterial, anti-fungal, anti-inflammatory, antiviral, anticancer, antioxidant, antimutagenic, and anti-diabetic activities.^[49] CAF and other cinnamic acid derivatives, such as coumaric acid and protocatechuic acid, have been identified in several beverages, including red wine, and they likely contribute to the putative cardiovascular-protective effects of high phenolic content alcoholic beverages.^[28] Desirably, the dietary should provide a good intake of antioxidants, including CAF. Food products changes in phenolic content in food products is considered an indicator in the food quality. Phenol content may decrease during storage and, in case of fresh food like fruit, phenol content decreases with fruit ripening.

CAF is abundant in coffee beans, whose content varies from ≈ 7 to 20 mg/100 g depending on the origin of the coffee and method of extraction.^[50] CAF is also present in many commercial beverages, like red wine (maximum value 430 μM)^[51] and fruit juices (maximum value 280 μM).^[52] Also, extra-virgin olive oil (EVO) contains CAF even if in modest contents (8.3 μM).^[53] These are all examples of food products having a CAF concentration range potentially detectable with the developed polyPCDA/ α -CD colorimetric sensor.

3. Conclusion

Herein, we investigated the color transition behaviors upon thermal stimulus and interaction with CDs of two PDAs obtained from DA monomers bearing either carboxylic (PCDA) or amino (PCDA-NH₂) polar heads. The change in the PDA polar head did not affect significantly vesicle size and thermo-chromatic transition. In both PDAs, color transition induced by thermal stimulus occurs straightforward between two distinct stable states and does not involve the disordering of the PDA crystal phase.

In contrast, the intermolecular forces among PDA polar heads affected PDA interaction with α -CD, which resulted more efficient for the diacetylene monomer PCDA than PCDA-NH₂. Presumably, the rigidity of the PCDA-NH₂ backbone induced by the establishment of two hydrogen bonds between head groups limits the formation of the inclusion complex. In general, the blue-to-red phase transition induced by α -CD interaction was complex and presumably affecting both PDA backbone conformation and interactions occurring among the individual PDA chains.

The polyPCDA/ α -CD assemblies were investigated as colorimetric sensors for the detection of food phenolic antioxidant compounds, Ty and CAF, by using the principle of competitive inclusion complex formation. The developed polyPCDA/ α -CD system was shown to be more sensitive to CAF than Ty, as evidenced by the rapid increase in CR' (%) already at low CAF concentrations. Reasonably, the α -CD better affinity for polyPCDA than Ty precluded the detection of this phenol. In contrast, an indirect colorimetric determination of CAF was demonstrated to be possible in concentration ranges suitable for different food products. Even if, at this stage, we were mainly interested in investigating the structure and color transition behavior of PDA/CD assemblies, the obtained results support the possibility to use this sys-

tem as sensor for monitoring the quality of food or valorization of agricultural byproducts, rich in phenolic antioxidants.

4. Experimental Section

Materials: 10,12-Pentacosadiynoic acid (PCDA, C₂₅H₄₂O₂, 374.60 g mol⁻¹), *N*-(3-dimethylaminopropyl)-*N'*-ethylcarbodiimide hydrochloride (EDC HCl), ethylenediamine (EDA), *N*-hydroxysuccinimide (NHS), α -cyclodextrin (α -CD), β -cyclodextrin (β -CD), sodium sulfate anhydrous, dichloromethane (CH₂Cl₂) were purchased from Sigma-Aldrich.

Synthesis of *N*-(2-Aminoethyl)-10,12-pentacosadiynamide: The synthesis of the amino-functionalized PCDA, *N*-(2-aminoethyl)-10,12-pentacosadiynamide (PCDA-NH₂), was performed as previously described with slight modifications.^[54] Briefly, 10 mL of a PCDA solution (50 mg, 0.13 mmol) in CH₂Cl₂, filtered by 0.7 μm PTFE syringe filters, were mixed with EDC HCl (41 mg, 0.26 mmol, EDC/PCDA molar ratio = 2:1). After EDC complete dissolution, NHS (20 mg, 0.17 mmol, NHS/PCDA molar ratio = 1.3:1) was added to the mixture and the reaction was kept at r.t. for 24 h. Synthesis of PCDA-NHS was followed by TLC using hexane:ethyl acetate:8:2 as eluent. The PCDA-NHS was purified by extraction in water to eliminate unreacted EDC and NHS and dried on sodium sulfate. The crude product was recovered after the solvent evaporation and finally purified by column chromatography using DCM as eluent. PCDA-NHS was characterized by ATR-FTIR and ¹H-NMR. For ¹H-NMR analysis, CDCl₃ was used as solvent.

¹H-NMR (300 MHz, CDCl₃) δ (ppm): 2.8 (s, 4H, CH₂CH₂), 2.6 (t, 2H, CH₂COOR), 2.2 (t, 4H, CH₂C \equiv C), 1.7 (m, 4H, CH₂CH₂COOR), 1.5 (m, 4H, CH₂CH₂C \equiv C), 1.4-1.2 (m, 26H, CH₂), 0.9 (t, 3H, CH₃).

PCDA-NH₂ was synthesized from PCDA-NHS active ester. PCDA-NHS (6.4 mg, 0.27 mmol) was dissolved in CH₂Cl₂ (20 mL) and added dropwise to a 5 mL solution of ED (2.7 mmol) in CH₂Cl₂. A 1:10 molar ratio between PCDA-NHS and EDA was chosen for the reaction. In this way, the synthesis of the mono-amide with a free amino group, i.e., PCDA-NH₂, is reasonably preferable to that of the symmetric amide (PCDA-NH-CH₂CH₂-NH-PCDA) bearing two sequences of PCDA. After few minutes from EDA addition, the reaction became opalescent, due to the formation of the desired amidic compound.^[55] The reaction was carried out for 6 h at r.t. in the dark and under magnetic stirring. PCDA-NH₂ was purified by extensive extraction in water, dried on sodium sulfate anhydrous and recovered by solvent evaporation. The pure product was characterized by means of ATR-FTIR and ¹H and ¹³C-NMR.

¹H-NMR (300 MHz, CDCl₃) δ (ppm): 6.0 (s, 1H, COONH), 3.3 (m, 2H, CH₂NH), 2.8 (m, 2H, CH₂NH₂), 2.3 – 2.1 (m, 6H, CH₂C \equiv C and CH₂COONH) 1.6 (m, 2H, CH₂CH₂COONH), 1.5 (m, 4H, CH₂CH₂C \equiv C), 1.4-1.2 (m, 26H, CH₂), 0.9 (t, 3H, CH₃).

The compound solubilized in DMSO and diluted in MeOH was injected in a ESI-MS/MS (6500 Qtrap SCIex) mass spectrometer. The electrospray ionization source was operated in negative ionization for PCDA and positive ionization for PCDA-NH₂.

C, N and H contents PCDA and PCDA-NH₂ were conducted by EA 1110 CHNS-O instrument to evaluate the nitrogen/carbon ratio after PCDA amidation.

Fourier Transform Infrared Spectroscopy (FTIR): FTIR analysis was performed in an Attenuated Total Reflection (ATR) by a Nicolet 6700 (Thermo Fisher Scientific, Waltham, MA, USA) equipped with a Golden Gate ATR accessory, at a resolution of 2 cm⁻¹ and co-adding 100 scans.

Thermal Analysis: Differential Scanning Calorimetry (DSC) analysis of the two diacetylene (DA) monomers was performed by a Mettler TA-3000 DSC apparatus. Thermograms were acquired at 10 °C min⁻¹ in the +25 to +150 °C temperature range, under N₂ flux. Thermogravimetric analysis (TGA) was carried out by employing a Mettler TG 50 thermobalance (Mettler Toledo, Columbus, OH, USA). The sample analysis was performed under N₂ flow, in the temperature range of 25–600 °C, by using a heating rate of 10 °C min⁻¹.

Preparation of PCDA and PCDA-NH₂ Vesicles and Photopolymerization: PCDA and PCDA-NH₂ vesicles were prepared the nanoprecipitation method. Specifically, polymers (4 mg) were dissolved in DMSO (1 mL) and added dropwise to deionized water (10 mL) under stirring (500 rpm) to at room temperature a final concentration of 0.4 mg/mL (1.1 mM) and left to evaporate for 2 h. After storage at 4 °C overnight, vesicles were photopolymerized at 254 nm for 20 min by UV lamp, thus obtaining a blue suspension of polydiacetylene (PDA) vesicles. Polymerized self-assembled DA monomers were named polyPCDA and polyPCDA-NH₂.

Dynamic Light Scattering (DLS) and Zeta Potential: Size and zeta potential of polyPCDA and polyPCDA-NH₂ vesicles were evaluated by DLS measurements using a Zetasizer Nano spectrometer (Malvern Instruments Ltd.) equipped with a 4 mW HeNe laser source (632.8 nm) at 25 °C.

Colorimetric Response of Vesicles upon Thermal Stimulus: To investigate the colorimetric response of vesicles upon thermal stimulus, the blue PDA suspensions (0.167 mM), either polyPCDA or polyPCDA-NH₂, were incubated in a water bath at increasing temperatures (from 20 to 60 °C) for 30 s, to induce blue-to-red color transitions.

Absorbance of the solutions was measured by UV-vis spectrometer (HP8452A, Hewlett Packard, Palo Alto, CA, USA) and the degree of the blue-to-red color transition was quantified by calculating the colorimetric response (CR, %):

$$CR \% = \frac{(B_0 - B_1)}{B_0} \times 100 \quad (1)$$

where $B = \frac{I_{\text{Blue}}}{I_{\text{Blue}} + I_{\text{Red}}}$. I_{Blue} is the absorbance at 640 nm while I_{Red} is the absorbance at 540 nm. B_0 is obtained for the unperturbed polymerized blue samples while B_1 after the thermal stimulus.^[56]

Colorimetric Response of PolyPCDA and PolyPCDA-NH₂ Vesicles upon α -CD or β -CD Interaction: In order to assess the effect of α -CD or β -CD concentrations on the structure and colorimetric response of vesicles, the PDA suspension (0.167 mM), either polyPCDA or polyPCDA-NH₂, was put in contact with increasing concentrations of cyclodextrin (1-20 mM). After standing for 1 h at room T, an increase in turbidity of the suspensions was observed related to the formation of the PDA-CD complex.^[57] For UV-vis analysis, the suspensions were centrifugated for 15 min at 3000 rpm.

The apparent dissociation constant (K_d) of the PDA-CD complexes was determined by plotting ΔA_{640} versus [CD], where $\Delta A_{640} = A_{640,0} - A_{640,i}$. $A_{640,0}$ and $A_{640,i}$ represent the absorbances of the suspension at 640 nm before and after interaction with the fixed CD concentration. The results were interpolated with the Hill equation:^[23]

$$\Delta A_{640} = \frac{\Delta A_{\text{max}}[CD]^n}{K_d^n + [CD]^n} \quad (2)$$

where ΔA_{max} is the maximum change in the absorbance, n is a fitting parameter and K_d is the apparent dissociation constant.

Synchrotron X-Ray Scattering: Synchrotron X-ray scattering data was collected at the SAXS beamline on BM29 at the European Synchrotron Radiation Facility (ESRF) of Grenoble, France. Measurements were conducted in a 0.025–6 nm⁻¹ q -range and a sample-detector distance of 2.867 m. The photon energy was 12.5 keV. The X-ray images were recorded with a Pilatus detector (Pilatus3 “M in vacuum”), calibrated with silver behenate. The scattering intensity was measured as a function of the scattering vector q , where $q = \frac{4\pi(\sin\theta)}{\lambda}$, with 2θ being the scattering angle and λ being the wavelength. Samples were measured in a 1 mm diameter quartz glass capillary. Data analysis was done with SASview and ATAS 3.2.1. Experimental intensities were background corrected.

Detection of Phenolic Antioxidants by PolyPCDA/ α -CD Vesicles: The polyPCDA/ α -CD complexes which showed the best colorimetric response were investigated as sensors for phenolic compounds. Specifically, the polyPCDA colorimetric response upon exposure to α -CD was affected by adding phenolic compounds as competitive guest molecules for CD.

Caffeic acid (CAF) and Tyrosol (Ty) were chosen as model guest molecules due to their known ability to form inclusion complexes with α -CD.^[48]

DSC was used to study the formation of α -CD/phenol complexes by following changes in thermal properties of the guest molecules as a result of inclusion complex formation.^[58] For the preparation of α -CD/phenol complexes, Ty (27.6 mg) was dissolved in 10 mL of water (20 mM) while CAF (36.0 mg) in 10 mL of a 55:45 water/ethanol mixture (20 mM). Then, aliquots of the phenol solutions were added to a water solution of α -CD such to obtain three phenol/ α -CD molar ratios (0.5, 1 and 2). The lyophilized powders were weighted (5 mg) and submitted to DSC analysis by a Mettler TA-3000 DSC apparatus. Thermograms were acquired at 10 °C min⁻¹ in the +25 to +150 °C temperature range, under N₂ flux.

The colorimetric response of polyPCDA/ α -CD systems in presence of the chosen phenols was investigated by using 8 mM α -CD concentration. Different concentrations of CAF and Ty were dissolved in the α -CD water solution. After 10 min, the polyPCDA suspension was added in to the α -CD/phenol solution such to have a final polyPCDA concentration of 0.167 mM. After 1 h, the system was centrifuged (15 min, 3000 rpm) and the supernatant was submitted to UV-vis spectroscopy.

The colorimetric response (CR' (%)) was used to quantify the remained blue phase which did not form inclusion complex with α -CD. CR' (%) increases when the phenolic compound has good ability in inhibiting the color transition induced by α -CD.

The CR' (%) is expressed as:

$$CR' \% = \frac{R_0 - R_1}{R_0} \times 100 \quad (3)$$

where $R = \frac{I_{\text{Red}}}{I_{\text{Blue}} + I_{\text{Red}}}$. R_0 is calculated in absence of phenol (free α -CD is the total concentration) and R_1 , in presence of increasing concentration of phenol. Therefore, CR' (%) considers an apparent colorimetric transition from red ($CR' = 0\%$) to blue ($CR' = 100\%$).^[24]

Supporting Information

Supporting Information is available from the Wiley Online Library or from the author.

Acknowledgements

R.S. and B.B. contributed equally to this work. The authors wish to thank Dr. Alessandra Del Giudice for performing the SAXS measurements carried out at the ESRF facilities in Grenoble, France. This project was funded under the National Recovery and Resilience Plan (NRRP), Mission 4 Component 2 Investment 1.3 – Call for tender No. 341 of 15/03/2022 of Italian Ministry of University and Research funded by the European Union – NextGenerationEU. Award Number: Project code PE0000003, Concession Decree No. 1550 of 11/10/2022 adopted by the Italian Ministry of University and Research, CUP D93C22000890001, Project title “Research and innovation network on food and nutrition Sustainability, Safety and Security – Working ON Foods” (ONFoods). Also, the Sapienza University of Rome supported the work (Project n. AR12218168959586).

Conflict of Interest

The authors declare no conflict of interest.

Data Availability Statement

The data that support the findings of this study are available from the corresponding author upon reasonable request.

Keywords

colorimetric sensors, cyclodextrins, food industry, polydiacetylenes

Received: April 4, 2023
Revised: May 31, 2023
Published online: June 17, 2023

- [1] K. Ariga, M. Nishikawa, T. Mori, J. Takeya, L. K. Shrestha, J. P. Hill, *Sci. Technol. Adv. Mater.* **2019**, *20*, 51.
- [2] P. Calandra, D. Caschera, V. Turco Liveri, D. Lombardo, *Colloids Surf. A, Physicochem. Eng. Asp.* **2015**, *484*, 164.
- [3] D. Pochan, O. Scherman, *Chem. Rev.* **2021**, *121*, 13699.
- [4] S. Yadav, A. K. Sharma, P. Kumar, *Front. Bioeng. Biotechnol.* **2020**, *8*, 127.
- [5] P. L. Jacob, L. A. Cantu Ruiz, A. K. Pearce, Y. He, J. C. Lentz, J. C. Moore, F. Machado, G. Rivers, E. Apebende, M. R. Fernandez, I. Francolini, R. Wildman, S. M. Howdle, V. Taresco, *Polymer* **2021**, *228*, 123912.
- [6] G. Du, D. Belic, A. Del Giudice, V. Alfredsson, A. M. Carnerup, K. Zhu, B. Nyström, Y. Wang, L. Galantini, K. Schillén, *Angew. Chem. Int. Ed. Engl.* **2022**, *61*, e202113279.
- [7] Y. Hou, L. Zou, Q. Li, M. Chen, H. Ruan, Z. Sun, X. Xu, J. Yang, G. Ma, *Mater. Today Bio.* **2022**, *15*, 100327.
- [8] J. Cautela, B. Stenqvist, K. Schillén, D. Belić, L. K. Månsson, F. Hagemans, M. Seuss, A. Fery, J. J. Crassous, L. Galantini, *ACS Nano* **2020**, *14*, 15748.
- [9] M. Whitesides George, B. Grzybowski, *Science* **2002**, *295*, 2418
- [10] V. K. Praveen, B. Vedhanarayanan, A. Mal, R. K. Mishra, A. Ajayaghosh, *Acc. Chem. Res.* **2020**, *53*, 496.
- [11] Y. Chang, N. Tang, H. Qu, J. Liu, D. Zhang, H. Zhang, W. Pang, X. Duan, *Sci. Rep.* **2016**, *6*, 23970.
- [12] Q. Xu, S. Lee, Y. Cho, M. H. Kim, J. Bouffard, J. Yoon, *J. Am. Chem. Soc.* **2013**, *135*, 17751.
- [13] X. Cao, A. Gao, J.-T. Hou, T. Yi, *Coord. Chem. Rev.* **2021**, *434*, 213792.
- [14] X. Chen, G. Zhou, X. Peng, J. Yoon, *Chem. Soc. Rev.* **2012**, *41*, 4610.
- [15] B. Yoon, S. Lee, J.-M. Kim, *Chem. Soc. Rev.* **2009**, *38*, 1958.
- [16] X. Qian, B. Städler, *Chem. Mater.* **2019**, *31*, 1196.
- [17] E. Lebègue, C. Farre, C. Jose, J. Saulnier, F. Lagarde, Y. Chevalier, C. Chaix, N. Jaffrezic-Renault, *Sensors* **2018**, *18*, 599.
- [18] E. Cho, S. Jung, *Molecules* **2018**, *23*, 107.
- [19] A. D. Tjandra, A.-H. Pham, R. Chandrawati, *Chem. Mater.* **2022**, *34*, 2853.
- [20] S. Hussain, R. Deb, S. Suklabaidya, D. Bhattacharjee, S. A. Hussain, *Mater. Today Proc.* **2022**, *65*, 2765.
- [21] M. Weston, A.-H. Pham, J. Tubman, Y. Gao, A. D. Tjandra, R. Chandrawati, *Mater. Adv.* **2022**, *3*, 4088.
- [22] J.-M. Kim, J.-S. Lee, J.-S. Lee, S.-Y. Woo, D. J. Ahn, *Macromol. Chem. Phys.* **2005**, *206*, 2299.
- [23] J. Brockgreitens, S. Ahmed, A. Abbas, *J. Incl. Phenom. Macrocycl. Chem.* **2015**, *81*, 423.
- [24] P. Anekthirakun, M. Sukwattanasinitt, T. Tuntulani, A. Imyim, *Spectrochim. Acta A, Mol. Biomol. Spectrosc.* **2013**, *111*, 91.
- [25] C. Santos-Buelga, A. M. González-Paramás, T. Oludemi, B. Ayuda-Durán, S. González-Manzano, *Adv. Food Nutr. Res.* **2019**, *90*, 183.
- [26] H. Zhang, J. Pu, Y. Tang, M. Wang, K. Tian, Y. Wang, X. Luo, Q. Deng, *Foods* **2022**, *11*, 3198.
- [27] M. B. Medina, *J. Agric. Food Chem.* **2011**, *59*, 1565.
- [28] R. Abu-Amsha, K. D. Croft, I. B. Puddey, J. M. Proudfoot, L. J. Beilin, *Clin. Sci.* **1996**, *91*, 449.
- [29] I. Gulcin, *Toxicology* **2006**, *217*, 213.
- [30] F. Crisante, V. Taresco, G. Donelli, C. Vuotto, A. Martinelli, L. D'Ilario, L. Pietrelli, I. Francolini, A. Piozzi, *Adv. Exp. Med. Biol.* **2016**, *901*, 25.
- [31] R. Di Benedetto, R. Vari, B. Scazzocchio, C. Filesi, C. Santangelo, C. Giovannini, P. Matarrese, M. D'archivio, R. Masella, *Nutr. Metab. Cardiovasc. Dis.* **2007**, *17*, 535.
- [32] N. Charoenthai, T. Pattanatornchai, S. Wacharasindhu, M. Sukwattanasinitt, R. Traiphol, *J. Colloid Interface Sci.* **2011**, *360*, 565.
- [33] Z. Yuan, C.-W. Lee, S.-H. Lee, *Angew. Chem. Int. Ed. Engl.* **2004**, *43*, 4197.
- [34] K. Kuriyama, H. Kikuchi, T. Kajiyama, *Langmuir* **1998**, *14*, 1130.
- [35] S. Okada, S. Peng, W. Spevak, D. Charych, *Acc. Chem. Res.* **1998**, *31*, 229.
- [36] D. N. Batchelder, *Contemp. Phys.* **1988**, *29*, 3.
- [37] A. Matsumoto, *Prog. React.* **2001**, *26*, 59.
- [38] V. Enkelmann, *Adv. Polym. Sci.* **1984**, *63*, 91.
- [39] J. Nuck, K. Sugihara, *Macromolecules* **2020**, *53*, 6469.
- [40] V. Dobrosavljevic, R. M. Strat, *Phys. Rev. B* **1987**, *35*, 2781.
- [41] I. S. Park, H. J. Park, W. Jeong, J. Nam, Y. Kang, K. Shin, H. Chung, J.-M. Kim, *Macromolecules* **2016**, *49*, 1270.
- [42] Y. Lifshitz, Y. Golan, O. Konovalov, A. Berman, *Langmuir* **2009**, *25*, 4469.
- [43] M. Schott, *J. Phys. Chem. B* **2006**, *110*, 15864.
- [44] A. J. Campbell, C. K. L. Davies, *Polymer* **1995**, *36*, 675.
- [45] J. Szejtli, *Chem. Rev.* **1998**, *98*, 1743.
- [46] A. Berman, D. J. Ahn, A. Lio, M. Salmeron, A. Reichert, D. Charych, *Science* **1995**, *269*, 515.
- [47] S. Goutelle, M. Maurin, F. Rougier, X. Barbaut, L. Bourguignon, M. Ducher, P. Maire, *Fundam. Clin. Pharmacol.* **2008**, *22*, 633.
- [48] R. Shiozawa, Y. Inoue, I. Murata, I. Kanamoto, *Asian J. Pharm. Sci.* **2018**, *13*, 24.
- [49] S. S. Damasceno, B. B. Dantas, J. Ribeiro-Filho, D. A. M. Araújo, J. G. M. Da Costa, *Curr. Pharm. Des.* **2017**, *23*, 3015.
- [50] I. Trandafr, V. Nour, M. E. Ionica, *Arch. Latinom. Nutr.* **2013**, *63*, 11.
- [51] J. Burns, P. T. Gardner, J. O'neil, S. Crawford, I. Morecroft, D. B. Mcphail, C. Lister, D. Matthews, M. R. Maclean, M. E. J. Lean, G. G. Duthie, A. Crozier, *J. Agric. Food Chem.* **2000**, *48*, 220.
- [52] A. Schieber, P. Keller, R. Carle, *J. Chromatogr. A* **2001**, *910*, 265.
- [53] M. S. Jiménez, R. Velarte, J. R. Castillo, *Food Chem.* **2007**, *100*, 8.
- [54] M. J. Shin, *Macromol. Res.* **2020**, *28*, 703.
- [55] S. Wacharasindhu, S. Montha, J. Boonyiseng, A. Potisatityueng, C. Phollookin, G. Tumchareon, M. Sukwattanasinitt, *Macromolecules* **2010**, *43*, 716.
- [56] D. H. Charych, J. O. Nagy, W. Spevak, M. D. Bednarski, *Science* **1993**, *261*, 585.
- [57] H. Choi, J. S. Choi, *Bull. Korean Chem. Soc.* **2013**, *34*, 3083.
- [58] R. Suzuki, Y. Inoue, Y. Tsunoda, I. Murata, Y. Isshiki, S. Kondo, I. Kanamoto, *J. Incl. Phenom. Macrocycl. Chem.* **2015**, *83*, 177.